Analysis of Stress Intensity Factors for Curved Cracks*

Nao-Aki NODA**, Kazuhiro ODA***
and Kazumitsu ISHII****

In this paper, numerical solution of hypersingular integral equations in curved-crack problems is presented. The stress fields induced by two kinds of standard sets of force doublets are used as fundamental solutions. Then, the problem is formulated as a system of integral equations with the singularity of the form r^{-2}. In the numerical calculation, two kinds of unknown functions are approximated by the products of the fundamental density functions and power series. The calculation shows that the present method gives rapidly converging numerical results for curved cracks under various geometrical conditions. In addition, a method of evaluation of the stress intensity factors for arbitrary-shaped curved cracks is proposed using the approximate replacement with a simple straight crack.

Key Words: Elasticity, Stress Intensity Factor, Body Force Method, Hypersingular Integral Equation Method, Curved Crack

1. Introduction

In the investigation of fatigue crack growth behavior based on linear fracture mechanics, it is quite important to calculate exactly the stress intensity factor of the crack for various geometric configurations. In the two-dimensional curved-crack problem, the solution for a circular-arc crack in an infinite plate was first presented by Sih et al.(1) using the stress function given by Muskhelishvili(2); however, Atluri et al.(3) and Cotterell and Rice(4) corrected the error in the expression of the solution. Ioakimidis and Theocaris(5) gave the numerical solutions of a circular-arc crack in an isotropic elastic half-plane. Chen et al.(6) analyzed crack problems of parabolic shape, sine shape and snake shape in an infinite plate. Other curved-crack problems have been analyzed by an approximate method using the first-order solution(4),(7) and using the solution of the circular-arc crack(8),(9). However, little attention has been given to the relationship between curvature at the tip of the curved crack and the stress intensity factor.

In the previous papers(10)-(13), numerical solution of the singular integral equations with higher singularity of the form r^{-2}, that is, so-called hypersingular integral equations, has been discussed. The various crack problems were shown to be solved with higher accuracy compared with those reported previously. In this study, the method is applied to the analysis of curved-crack problems. As a basic model, the problem of a crack that consists of a straight part and a circular-arc part is treated. The calculation is carried out for the curved crack under various geometrical conditions in order to investigate the effect of curvature at the crack tip on the stress intensity factor. In addition, a method of evaluation of the stress intensity factors for arbitrary-shaped curved cracks is proposed using the approximate replacement with a simple straight crack.

* Received 16th September, 1993. Paper No. 92-1152
** Department of Mechanical Engineering, Kyushu Institute of Technology, 1-1 Sensui-cho, Tobata-ku, Kitakyushu 804, Japan
*** Graduate School, Kyushu Institute of Technology
**** Isuzu Engineering Co., Ltd., 8 Tuchitana, Fujisawa, Kanagawa 252, Japan

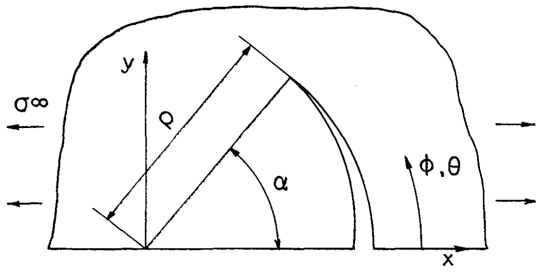

Fig. 1 Circular-arc edge crack in a semi-infinite plate under uniform tension

2. Numerical Solution of Singular Integral Equation

In this section, using the example of the tension of a semi-infinite plate with a circular-arc edge crack (Fig. 1), a method of solution will be explained. This problem can be solved by using the stress field induced by two kinds of standard sets of force doublets in a semi-infinite plate as a fundamental solution, on the basis of the principle of superposition[(10)-(13)]. The problem is reduced to the following integral equation, where the densities of the body force doublets (continuously distributed pairs of point forces) along the imaginary boundary of the crack, tension type $f_1(\phi)$ and shear type $f_2(\phi)$, are the unknown functions.

$$\begin{aligned}&\int_0^\alpha h_{11}(\phi,\theta)f_1(\phi)d\phi+\int_0^\alpha H_{11}(\phi,\theta)f_1(\phi)d\phi\\&+\int_0^\alpha h_{12}(\phi,\theta)f_2(\phi)d\phi+\int_0^\alpha H_{12}(\phi,\theta)f_2(\phi)d\phi\\&=-\sigma^\infty\cos^2\theta \qquad (1\cdot\mathrm{a})\end{aligned}$$

$$\begin{aligned}&\int_0^\alpha h_{21}(\phi,\theta)f_1(\phi)d\phi+\int_0^\alpha H_{21}(\phi,\theta)f_1(\phi)d\phi\\&+\int_0^\alpha h_{22}(\phi,\theta)f_2(\phi)d\phi+\int_0^\alpha H_{22}(\phi,\theta)f_2(\phi)d\phi\\&=\sigma^\infty\sin\theta\cos\theta \qquad (1\cdot\mathrm{b})\end{aligned}$$

Equation (1) is basically the boundary conditions on the imaginary boundary ; that is, $\sigma_n=0$, $\tau_{nt}=0$. Here, $h_{ij}(\phi,\theta)$ $(i,j=1,2)$ is stresses due to the standard set of force doublets in an infinite plate and $H_{ij}(\phi,\theta)$ is the function known to satisfy the boundary condition except at the crack surface.

In the numerical solution of Eq. (1), the unknown function $f_i(\phi)$ $(i=1,2)$ is approximated by the product of the fundamental density function $w_i(\phi)$ and the power series ϕ^n :

$$f_1(\phi)=F_{\mathrm{I}}(\phi)w_1(\phi),\quad F_{\mathrm{I}}(\phi)\cong\sum_{n=0}^{N-1}a_n\phi^n,$$

$$w_1(\phi)=\frac{(\kappa+1)^2\sigma^\infty}{2(\kappa-1)}\rho\sqrt{\alpha^2-\phi^2}, \qquad (2\cdot\mathrm{a})$$

$$f_2(\phi)=F_{\mathrm{II}}(\phi)w_2(\phi),\quad F_{\mathrm{II}}(\phi)\cong\sum_{n=0}^{N-1}b_n\phi^n,$$

$$w_2(\phi)=\frac{(\kappa+1)\sigma^\infty}{2}\rho\sqrt{\alpha^2-\phi^2}, \qquad (2\cdot\mathrm{b})$$

where N is the number of collocation points, $\kappa=3-4\nu$ plane strain, and ν Poisson's ratio.

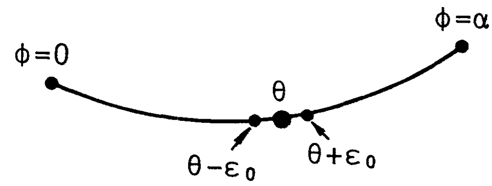

Fig. 2 Division of the integration interval

Using the above approximation method, the problem is reduced to determining the coefficients a_n and b_n in Eq. (2). A convenient set of collocation points is given by

$$\theta_j=\frac{\alpha}{2}\cos\left(\frac{2j-1}{N}\frac{\pi}{2}\right)+\frac{\alpha}{2},\quad (j=1,2,\cdots,N). \qquad (3)$$

The stress intensity factor can be calculated from

$$K_{\mathrm{I,II}}=F_{\mathrm{I,II}}(\alpha)\sigma^\infty\sqrt{\pi\rho\alpha}. \qquad (4)$$

The method presented in this section can be applied to various curved-crack problems. As an example, a crack that consists of a straight part and a circular-arc part is considered in this study. The boundary conditions along the straight part of the crack are satisfied by the product of the fundamental density functions and Chebyshev polynomials, as we have already described in Refs. (10)-(13).

3. Evaluation of Singular Integral

The integration of the first and the third terms on the left-hand side of Eq. (1) involves singular terms. In the analysis of straight-crack problems, this type of singular integral is easily evaluated by using the formula of Chebyshev polynomials[(10)-(13)]. In the curved-crack problem, however, no convenient formula is available; therefore, the following method of evaluation of singular integrals is applied[(14)].

The integration interval is divided into three parts as shown in Fig. 2.

$$\begin{aligned}I&=\int_0^\alpha h(\phi,\theta)f(\phi)d\phi\\&=\int_0^{\theta-\varepsilon_0}h(\phi,\theta)f(\phi)d\phi\\&+\int_{\theta-\varepsilon_0}^{\theta+\varepsilon_0}h(\phi,\theta)f(\phi)d\phi\\&+\int_{\theta+\varepsilon_0}^{\alpha}h(\phi,\theta)f(\phi)d\phi\\&=I_1+I_2+I_3 \qquad (5)\end{aligned}$$

The first and the third integrals having no singular term can be easily evaluated through the numerical integration procedure. By substituting $\phi=\theta+\varepsilon$, the second integral can be expressed as a power series of ε, as shown in Eq. (6).

$$\begin{aligned}I_2&=\int_{-\varepsilon_0}^{\varepsilon_0}h(\theta+\varepsilon,\theta)f(\theta+\varepsilon)d\varepsilon\\&=\int_{-\varepsilon_0}^{\varepsilon_0}\left(\frac{c_1}{\varepsilon^2}+\frac{c_2}{\varepsilon}+c_3+\cdots\right)d\varepsilon \qquad (6)\end{aligned}$$

Table 1 Convergency of the SIF for circular-arc crack obtained by the conventional body force method ($k_{I,II}=K_{I,II}/\sigma^\infty\sqrt{\rho}$)

N	α=30.0 β=0.0		α=30.0 β=30.0			
	$k_{IA,B}$	$k_{IIA,B}$	k_{IA}	k_{IIA}	k_{IB}	k_{IIB}
30	0.97846	0.57695	1.1603	0.058016	0.38559	0.78451
50	0.97650	0.58114	1.1620	0.053928	0.38177	0.78581
80	0.97559	0.58322	1.1630	0.051956	0.37990	0.78652
100	0.97534	0.58386	1.1632	0.051378	0.37935	0.78675
150	0.97506	0.58463	1.1636	0.050697	0.37869	0.78706
200	0.97495	0.58497	1.1638	0.050409	0.37840	0.78722
∞(100-150)	0.97450	0.58517	1.1644	0.049336	0.37736	0.78769
∞(150-200)	0.97463	0.58601	1.1644	0.049543	0.37754	0.78768
Exact	0.97496	0.58562	1.1643	0.050048	0.37797	0.78768

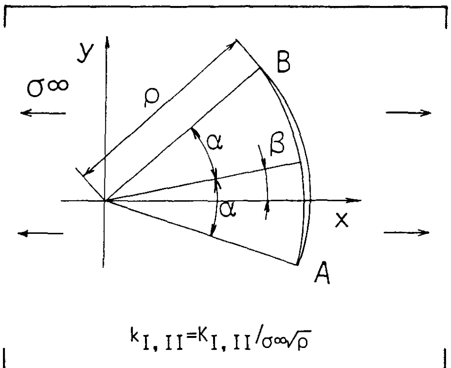

Table 2 Convergency of the SIF for circular-arc crack obtained by the present method ($k_{I,II}=K_{I,II}/\sigma^\infty\sqrt{\rho}$)

N	α=30.0 β=0.0		α=30.0 β=30.0			
	$k_{IA,B}$	$k_{IIA,B}$	k_{IA}	k_{IIA}	k_{IB}	k_{IIB}
2	0.9895561	0.5619829	1.151651	0.05946876	0.4074583	0.7688413
4	0.9749634	0.5856141	1.164283	0.05005156	0.3779830	0.7876736
6	0.9749593	0.5856211	1.164287	0.05004821	0.3779741	0.7876775
8	0.9749593	0.5856211	1.164287	0.05004820	0.3779741	0.7876775
10	0.9749593	0.5856212	1.164287	0.05004821	0.3779741	0.7876775
Exact	0.9749593	0.5856211	1.164287	0.05004821	0.3779741	0.7876775

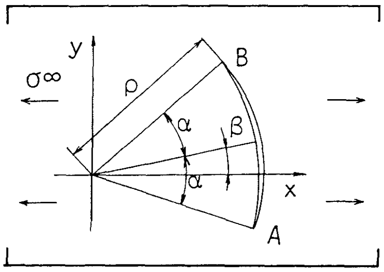

The first integral term on the right-hand side in Eq. (6) can be evaluated as the finite-part integral proposed by Hadamard[15]. Since the second term is an odd function, Cauchy's principal value of the integral should be zero. Neglecting the terms of higher order than ε_0^2, we obtain

$$I_2 \cong -\frac{2c_1}{\varepsilon_0}+2c_3\varepsilon_0. \qquad (7)$$

Then the singular integrals are calculated by determining the coefficients c_1 and c_3 in Eq. (6).

4. Numerical Results and Discussion

4.1 Circular-arc crack in an infinite plate

The accuracy of the result obtained by the present method is verified through comparison with the exact solution of the circular-arc crack. In addition, the convergency of the results is compared with that of the conventional numerical method.

Table 1 shows the stress intensity factors calculated by the conventional body force method. In solving the integral equation (1) for the conventional method, the imaginary crack line is divided into N equal intervals, and the unknown functions $f_1(\phi)$ and $f_2(\phi)$ are approximated by the fundamental density function and the stepped function which take constant values in each interval. Here, the symbol ∞(100-150) in Table 1 designates the extrapolated value using the results of $N=100$ and 150 on the basis of the linear relationship between the SIF and $1/N$. As shown in Table 1, the results obtained by the conventional method using the stepped function coincide with the exact solution to 3 digits. In contrast, Table 2 shows the results obtained by the present method, which coincide with the exact solution to all 7 digits when $N=6$ without extrapolation. It is found that the present method gives a rapidly converging numerical result with short CPU time for curved-crack problems.

4.2 Curved crack in infinite plate

To investigate the effect of curvature at the crack tip on the stress intensity factor, a curved crack that consists of a straight part and a circular-arc part is considered as a basic crack model. In Table 3, dimensionless SIFs at crack tip B for various values of the relative curvature $\rho/2c$ and the angle α are shown, where $2c$ is the projected length of the total crack in the direction perpendicular to the tensile axis. To find an estimation method of the SIF for an arbitrary-shaped curved crack in an actual structure, the present results are compared with the SIF of the straight crack with the same inclination angle α and with the same projected length $2c$, as shown in Fig. 3. As shown in Table 3, the value of F_I at tip B of the curved crack can be estimated from that of the straight crack with error less than about 4% when $\rho/2c \geqq 0.2$ and $\alpha \leqq 45°$. On the other hand, the difference in the values of F_{II} between the curved and the straight crack is

Table 3 Dimensionless SIF of a crack that consists of a straight part and circular-arc part ($F_{I,II}=K_{I,II}/\sigma^{\infty}\sqrt{\pi c}$)

α \ ρ/2c	15.0 F_I	15.0 F_{II}	30.0 F_I	30.0 F_{II}	45.0 F_I	45.0 F_{II}	60.0 F_I	60.0 F_{II}
0.1	0.9656	0.1616	0.8547	0.3257	0.6746	0.4571	0.4480	0.5327
0.2	0.9623	0.1741	0.8389	0.3557	0.6387	0.5006	0.3890	0.5820
0.4	0.9581	0.1907	0.8207	0.3934	0.6009	0.5532	0.3338	0.6386
0.6	0.9554	0.2024	0.8100	0.4183	0.5826	0.5847	0.3141	0.6675
0.8	0.9533	0.2116	0.8034	0.4361	0.5742	0.6042	0.3110	0.6797
1.0	0.9517	0.2190	0.7992	0.4492	0.5718	0.6152	0.3165	0.6805
Straight	0.9493	0.2544	0.8059	0.4653	0.5946	0.5946	0.3536	0.6124

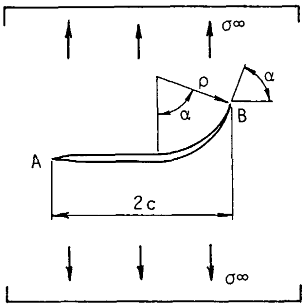

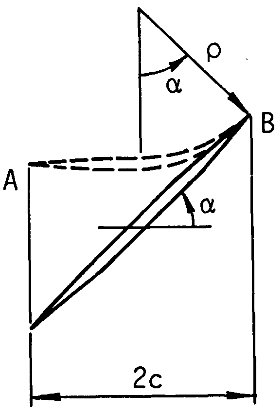

Fig. 3 Estimation of the SIF using the approximate replacement with a straight crack

comparatively large.

4.3 Circular-arc edge crack in a semi-infinite plate

The circular-arc edge crack in a semi-infinite plate under uniform tension is considered. First, the problem of circular-arc edge crack, in which the tangent direction at the crack tip is perpendicular to the half-plane boundary, is analyzed. The dimensionless SIFs for various values of α obtained by the present analysis are shown compared with the results of Ioakimidis and Theocaris[5] in Table 4. The two sets of results almost coincide with each other. In Table 4, F_I^* is the dimensionless SIF based on $\sigma^{\infty}\sqrt{\pi b}$, where $b=\rho\sin\alpha$ is the projected crack length. The values of F_I^* are in close agreement with the well-known value, 1.1215.

Next, other shapes of circular-arc edge cracks shown in Fig. 1 are analyzed. Table 5 shows the convergency of the SIFs. It is found that the convergency of the present results is extremely good for edge cracks as well as for internal cracks. In Table 6, the dimensionless SIFs for various values of α are shown in comparison with the SIFs for an oblique edge crack. The angle of the oblique edge crack is chosen to have the same angle of the tangent direction

Table 4 Dimensionless SIF of the circular-arc edge crack, in which the tangent of the crack tip is perpendicular to the half-plane boundary ($F_I=K_I/\sigma^{\infty}\sqrt{\pi\rho\alpha}$, $F_I^*=K_I/\sigma^{\infty}\sqrt{\pi b}$, $b=\rho\sin\alpha$)

α	Present analysis F_I	(F_I^*)	Ioakimidis and Theocaris [5] F_I
15.0	1.1152	(1.1216)	1.115
30.0	1.0962	(1.1218)	1.100
45.0	1.0647	(1.1221)	1.065
60.0	1.0206	(1.1223)	1.023
75.0	0.9642	(1.1224)	0.965

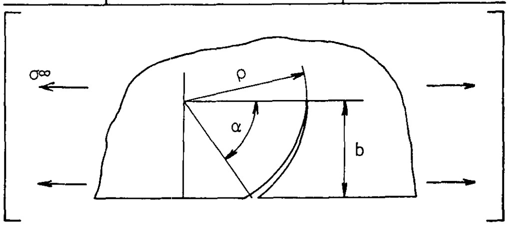

Table 5 Convergency of the SIF for the circular-arc edge crack in Fig. 1

N	α = 30.0 F_I	α = 30.0 F_{II}	α = 60.0 F_I	α = 60.0 F_{II}
4	0.920717	0.304933	0.463699	0.352683
6	0.919676	0.305050	0.462889	0.352426
8	0.919664	0.305088	0.462765	0.352481
10	0.919671	0.305095	0.462749	0.352493
12	0.919675	0.305096	0.462747	0.352496
14	0.919677	0.305097	0.462747	0.352496

at the tip of the circular-arc edge crack as shown in Fig. 4. As shown in Table 6, it can be seen that Mode I SIFs of the straight crack conform more closely to those of the circular-arc crack for a wide range of α. The values of F_{II} of the oblique edge crack are also in good agreement, within 5%, for $\alpha\leqq 60°$.

4.4 Curved edge crack in a semi-infinite plate

Finally, the edge crack that consists of a straight part and a circular-arc part is considered as a basic model of a curved edge crack. The SIFs are calculated for various values of α and c_2/c_1, where α is the

Table 6 Comparison of the SIF between the circular-arc crack and the oblique edge crack ($F_{I,II}=K_{I,II}/\sigma^{\infty}\sqrt{\pi b}$, $b=\rho\tan\alpha$)

α	Present analysis F_I	Present analysis F_{II}	Straight F_{Is}	Straight F_{IIs}	F_I/F_{Is}	F_{II}/F_{IIs}
15.0	1.0684	0.1720	1.0686	0.1738	0.9998	0.9896
30.0	0.9197	0.3051	0.9201	0.3058	0.9996	0.9977
45.0	0.7044	0.3699	0.7049	0.3645	0.9993	1.0148
60.0	0.4627	0.3525	0.4625	0.3362	1.0004	1.0485
75.0	0.2345	0.2540	0.2318	0.2261	1.0112	1.1234

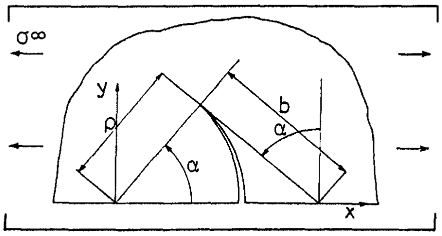

Table 7 Dimensionless SIF of an edge crack that consists of a straight part and circular-arc part ($F_{I,II}=K_{I,II}/\sigma^{\infty}\sqrt{\pi b}$, $b=c_1/\cos\alpha$)

c_2/c_1 \ α	15.0 F_I	15.0 F_{II}	30.0 F_I	30.0 F_{II}	45.0 F_I	45.0 F_{II}	60.0 F_I	60.0 F_{II}
0.1	1.0697	0.1604	0.9240	0.2873	0.7117	0.3541	0.4707	0.3465
0.2	1.0689	0.1649	0.9212	0.2950	0.7065	0.3629	0.4639	0.3539
0.4	1.0685	0.1690	0.9197	0.3015	0.7040	0.3692	0.4613	0.3573
0.6	1.0684	0.1706	0.9196	0.3037	0.7040	0.3704	0.4618	0.3562
0.8	1.0684	0.1715	0.9196	0.3047	0.7042	0.3703	0.4624	0.3543
1.0	1.0684	0.1720	0.9197	0.3051	0.7044	0.3699	0.4627	0.3525
Straight	1.0686	0.1738	0.9201	0.3058	0.7049	0.3645	0.4625	0.3362

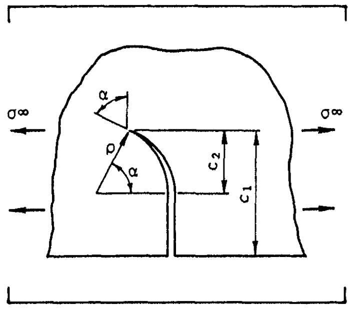

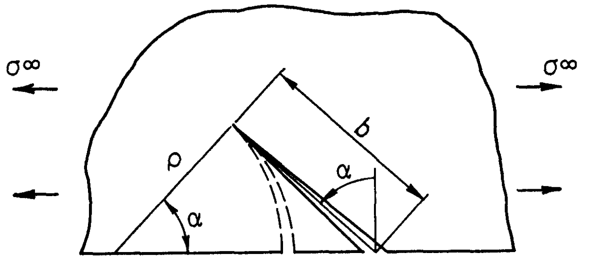

Fig. 4 Oblique edge crack with the same inclination angle at the tip of the circular-arc edge crack

angle of the crack tip, c_1 is the projected crack length, and $c_2=\rho\sin\alpha$ is the projected length of the circular-arc part. The dimensionless SIFs are shown in Table 7 in comparison with the SIFs for the oblique edge crack having the same inclination angle α. As shown in Table 7, it can be seen that Mode I SIFs of the straight crack are in close agreement with those of the curved edge crack for wide ranges of α and c_2/c_1. The difference between Mode II SIFs for curved and straight edge cracks is generally small, except in the case of large α and small c_2/c_1.

In the case of the edge crack, it is found that the curvature of the crack tip does not have much effect on the stress intensity factor. The approximate SIF for an arbitrary-shaped curved edge crack can be evaluated by the replacement with a straight edge crack, if the inclined angle at the crack tip and the projected crack length are given.

5. Conclusions

In this paper, numerical solution of the hyper-singular integral equation in curved crack problems was considered. Numerical calculations were carried out for curved cracks under various geometrical conditions, and the effect of curvature at the crack tip on the stress intensity factor was discussed. The conclusions are summarized as follows.

(1) In the present method, the unknown functions are approximated by the product of the fundamental density function and power series. The convenient formula such as the Chebyshev polynomial, which is useful for straight crack problems, cannot be applied to curved crack problems; thus, the singular integral was evaluated from the expansion of the integrand. It was found that the present method gives good convergency of the numerical results. In particular, the present result of the circular-arc crack in an infinite plate under uniform tension coincided with the exact solution to 7 digits.

(2) The curved crack that consists of a straight part and a circular-arc part in an infinite plate was considered as the basic crack model. The dimensionless SIFs at curved crack tip B for various values of the relative radius of curvature $\rho/2c$ and the angle α were shown in Table 3. The present results were compared with the SIF of the straight crack with the same inclination angle and the same projected length (see Fig. 3). The Mode I SIF of an arbitrary-shaped curved crack can be approximately given by that of

the simple equivalent straight crack when $\rho/2c \geqq 0.2$ and $\alpha \leqq 45°$. On the other hand, the difference in Mode II SIF between the curved and the straight crack is comparatively large.

(3) The curved edge crack that consists of a straight part and a circular-arc part in a semi-infinite plate was considered. The dimensionless SIFs for the curved edge crack were shown in comparison with the SIFs for an oblique edge crack. In the case of edge crack, it was found that the curvature at the crack tip does not have much effect on the stress intensity factor. The SIF for an arbitrary-shaped curved edge crack can therefore be evaluated by that of the straight edge crack with the same inclined angle and the same projected length as the curved crack.

References

(1) Sih, G.C., Paris, P.C. and Erdogan, F., Crack Tip Stress Intensity Factors for Plane Bending Problems, Trans. ASME, Ser. E, J. Appl. Mech., Vol. 29, (1962), p. 306.

(2) Muskhelishvili, N.I., Some Basic Problems of the Mathematical Theory of Elasticity, 4th ed., Noordhoff, Groningen, The Netherlands, (1963), p. 531.

(3) Atluri, S.N., Kobayashi, A.S. and Nakagaki, M., An Assumed Displacement Hybrid Finite Element Model for Linear Fracture Mechanics, Int. J. Fract., Vol. 11, No. 2, (1975), p. 257.

(4) Cotterell, B. and Rice, J.R., Slightly Curved or Kinked Cracks, Int. J. Fract., Vol. 16, No. 2, (1980), p. 155.

(5) Ioakimidis, N.I. and Theocaris, P.S., A System of Curvilinear Cracks in an Isotropic Elastic Half-Plane, Int. J. Fract., Vol. 15, No. 4, (1979), p. 299.

(6) Chen, Y.Z., Gross, D. and Huang, Y.J., Numerical Solution of the Curved Crack Problems by Means of Polynomial Approximation of the Dislocation Distribution, Eng. Fract. Mech., Vol. 39, No. 5, (1991), p. 791.

(7) Sumi, Y., Nemat-Nasser, S. and Keer, L.M., On Crack Branching and Curving in a Finite Body, Int. J. Fract., Vol. 21, (1983), p. 67.

(8) Leevers, P.S., Radon, J.C. and Culver, L.E., Fracture Trajectories in a Biaxially Stressed Plate, J. Mech. Phys. Solids, Vol. 24, (1976), p. 381.

(9) Alpa, G., Bozzo, E. and Gambarotta, L., Some Observations on the Path Stability in Fracture Propagation for Biaxially Stressed Plates, Eng. Fract. Mech., Vol. 13, (1980), p. 791.

(10) Noda, N.-A., Umeki, H. and Erdogan, F., The Singular Integral Equation Method in the Analysis of a Crack Perpendicular to the Interface (The Hypersingular Integral Equation Method and the Body Force Method), Trans. Jpn. Soc. Mech. Eng., (in Japanese), Vol. 55, No. 520, A(1989), p. 2521.

(11) Noda, N.-A., Oda, K. and Chen, D.H., The Hypersingular Integral Equation Method in the Analysis of Mixed Mode Crack Problems (The Extended Body Force Method Using Chebyshev Polynomials), Trans. Jpn. Soc. Mech. Eng., (in Japanese), Vol. 56, No. 532, A(1990), p. 2405.

(12) Noda, N.-A., Oda, K. and Masuda, C., The Hypersingular Integral Equation Method in the Analysis of Bent and Branched Cracks, Trans. Jpn. Soc. Mech. Eng., (in Japanese), Vol. 57, No. 542, A (1991), p. 232.

(13) Noda, N.-A. and Oda, K., Numerical Solution of the Singular Integral Equations in the Crack Analysis Using the Body Force Method, Int. J. Fract., Vol. 58, (1992), p. 285.

(14) Nisitani, H., The Two-Dimensional Stress Problem Solved Using an Electric Digital Computer, J. Jpn. Soc. Mech. Eng., (in Japanese), Vol. 70, No. 580, (1967), p. 627. [Bull. Jpn. Soc. Mech. Eng., Vol. 11, (1968), p. 14.]

(15) Hadamard, J., Lectures on Cauchy's problem in linear partial differential equations, (1923), Yale University Press.